CONVERGENT ERROR-CONTROLLED MESH ADAPTATION

G. Brèthes*, A. Loseille, F. Alauzet**, Alain Dervieux***

(*)INRIA - projet Ecuador Sophia-Antipolis, France
(**)INRIA - projet Gamma Rocquencourt, France
gautier.brethes@inria.fr

June 5, 2015

Motivations

$$-div(\alpha \nabla u) = f$$

We want a computational effort as small as possible.
Related to the discrete system size, *i.e.* the number of degrees of freedom:

- Reduce the number of operations per degree of freedom: FMG,
- Reduce the number of degrees of freedom: mesh adaptation.

Talk contents

- Hessian-based adaptation
- Goal-oriented adaptation
- Norm-oriented adaptation
- Applications with adaptive FMG

I. Hessian-based mesh adaptation

Mesh parameterization

Metric $\mathcal{M}$: $\mathcal{M}(\mathbf{x}) = \mathcal{R}^t(x,y)\begin{pmatrix} \frac{1}{\Delta\xi^2(x,y)} & 0 \\ 0 & \frac{1}{\Delta\eta^2(x,y)} \end{pmatrix}\mathcal{R}(x,y)$

with:

$\Delta\xi(x,y) =$ mesh size in the first characteristic direction

$\Delta\eta(x,y) =$ mesh size in the second characteristic direction

$\mathcal{R}(x,y) =$ matrix of eigenvectors.

Number of vertices: $\mathcal{C}(\mathcal{M}) = \int_\Omega \sqrt{det(\mathcal{M}(\mathbf{x}))}\,\mathrm{d}\mathbf{x}$

Riemannian distance between two points:

$$dist(\mathbf{a},\mathbf{b}) = length_{\mathcal{M}}(\mathbf{ab}) = \int_0^1 \sqrt{{}^t\mathbf{ab}\mathcal{M}(\mathbf{a}+\theta\mathbf{ab})\mathbf{ab}}\,\mathrm{d}\theta$$

Which mesh?

$\mathcal{H}_{\mathcal{M}}$ =**unit mesh for $\mathcal{M}$** $\Leftrightarrow \forall$ edge $\mathbf{e} \in \mathcal{H}_{\mathcal{M}}$, $length_{\mathcal{M}}(\mathbf{e}) \approx 1$

Minimize the **interpolation error**:

$\epsilon_{\mathcal{M}} = ||u - \Pi_{\mathcal{M}} u|| \approx \mathrm{trace}(\mathcal{M}^{-\frac{1}{2}}(\mathbf{x})\,|H_u(\mathbf{x})|\,\mathcal{M}^{-\frac{1}{2}}(\mathbf{x}))$

under the constraint: $\mathcal{C}(\mathcal{M}) = \int_\Omega \sqrt{\det(\mathcal{M}_{L^1}(\mathbf{x}))}\,\mathrm{d}\mathbf{x} = N.$

The **optimal metric field** $\mathcal{M}_{L^1}(\mathbf{x})$ is given by:

$$\mathcal{M}_{L^1,opt}(\mathbf{x}) = \mathcal{K}_1(1, u_{\mathcal{M}})$$

$$\mathcal{K}_1(k, u_{\mathcal{M}}) = \mathcal{D}_{L^1} det(|kH_{u_{\mathcal{M}}}(\mathbf{x})|)^{\frac{-1}{5}} |kH_{u_{\mathcal{M}}}(\mathbf{x})|$$

$$\mathcal{D}_{L^1} = N^{\frac{2}{3}}\left(\int_\Omega det(|kH_{u_{\mathcal{M}}}(\mathbf{x})|)^{\frac{2}{5}}\ \mathrm{d}\mathbf{x}\right)^{\frac{-2}{3}}.$$

The Hessian based method doesn't take into account the PDE.

G. Brèthes, O. Allain, and A. Dervieux. A mesh-adaptative metric-based Full-Multigrid for the Poisson problem. to appear in I.J. Numer. Meth. Fluids, 2015. pre-print: http://www-sop.inria.fr/members/Gautier.Brethes/article-ADA-MG.pdf

II.Goal-Oriented mesh adaptation

The goal-oriented formulation is probably the first formulation in which the mesh adaptation problem is completely set on a mathematical form:
Find the mesh which minimizes the error committed on a specified scalar output:

$$\min_{\mathcal{M}} \delta j_{goal}(\mathcal{M}) = \left|(g, \Pi_{\mathcal{M}} u - u_{\mathcal{M}})\right| \,,\; \mathcal{C}(\mathcal{M}) = N.$$

A. LOSEILLE, A. DERVIEUX and F. ALAUZET, Fully anisotropic goal-oriented mesh adaptation for 3D steady Euler equations, Journal of Computational Physics, Vol. 229, Issue 8, pp. 2866-2897, 2010.

Goal-Oriented mesh adaptation

$$\delta j_{goal}(\mathcal{M}) = |(g, \Pi_{\mathcal{M}} u - u_{\mathcal{M}})|.$$

After introduction of an **adjoint**

$$\delta j_{goal}(\mathcal{M}) \approx a(\Pi_{\mathcal{M}} u - u_{\mathcal{M}}, u^*_{g,\mathcal{M}})$$

with $a(.,.) = (\alpha \nabla ., \nabla .)$
Expression $\Pi_{\mathcal{M}} u - u_{\mathcal{M}}$ needs be replaced by an **estimate**:

$$a(\Pi_{\mathcal{M}} u - u_{\mathcal{M}}, \varphi) \ \preceq \ K \int_{\Omega} |\rho(H(\varphi)| \ |u - \Pi_{\mathcal{M}} u| \mathrm{d}\mathbf{x}$$

$$|\delta j_{goal}(\mathcal{M})| \ \preceq \ K \int_{\Omega} |\rho(H(u^*_{g,\mathcal{M}})| \ |u - \Pi_{\mathcal{M}} u| \mathrm{d}\mathbf{x}$$

by *freezing* $\rho(H(u^*_{g,\mathcal{M}})$ with respect to $\mathcal{M}$. Then:

$$\mathcal{M}_{opt,goal} = \mathcal{K}_1(|\rho(H(u^*_{g,\mathcal{M}}))|, u_{\mathcal{M}}).$$

Goal-Oriented mesh adaptation

Step 1:

$$a(\psi, u^*_{g,\mathcal{M}}) = |(g, \psi)|$$

Step 2:

$$\mathcal{M}_{opt,goal} = \mathcal{K}_1(|\rho(H(u^*_{g,\mathcal{M}}))|, u_{\mathcal{M}})$$

But:
- only features influencing the functional will be refined,
- then we have lost the convergence to the PDE solution!

III. Norm-Oriented mesh adaptation

Minimize:

$$j(\mathcal{M}) = ||\Pi_{\mathcal{M}} u - u_{\mathcal{M}}||^2_{L^2(\Omega)}$$

Term $\Pi_{\mathcal{M}} u - u_{\mathcal{M}}$ is approximated by a *corrector* u'_{DeC} obtained by **coarse-fine Defect Correction**:

$$u_h = A_h^{-1} f_h \ \ , \ \ u_{h/2} = A_{h/2}^{-1} f_{h/2} \quad \Rightarrow \quad u_{h/2} - u_h \approx \frac{3}{4}(u - u_h)$$

Computing $A_{h/2}^{-1} f_{h/2}$ is expensive, define instead:

$$u'_{DeC} = A_h^{-1} \frac{4}{3} R_{h/2 \to h}(A_{h/2} P_{h \to h/2} u_h - f_{h/2})$$

where the residual transfer $R_{h/2 \to h}$ accumulates on coarse grid vertices the values at fine vertices in neighboring coarse elements multiplied with barycentric weights and $P_{h \to h/2}$ linearly interpolates coarse values on fine mesh.

Norm-Oriented Adaptation

Functional:

$$j(\mathcal{M}) \approx |u'_{DeC}|^2 \approx (u'_{DeC}, \Pi_{\mathcal{M}} u - u_{\mathcal{M}})$$

We freeze $g = u'_{DeC}$ and get a goal-oriented formulation.
Adjoint:

$$a(\psi, u^*_{DeC}) = (u'_{DeC}, \psi)$$

Like with the goal-oriented:

$$\mathcal{M}_{opt,norm} = \mathcal{K}_1(|\rho(H(u^*_{DeC}))|, u_{\mathcal{M}})$$

Step 1:

$$u'_{DeC} = A_h^{-1}\frac{4}{3}R_{h/2\to h}(A_{h/2}P_{h\to h/2}u_h - f_{h/2})$$

Step 2:

$$a(\psi, u^*_{DeC}) = (\psi, u'_{DeC})$$

Step 3:

$$\mathcal{M}_{opt,norm} = \mathcal{K}_1(|\rho(H(u^*_{DeC}))|, u_{\mathcal{M}})$$

Convergence to the PDE solution

Three metrics

$$\mathcal{K}_1(k, u_{\mathcal{M}}) = \mathcal{D}_{L^1} det(|kH_{u_{\mathcal{M}}}(\mathbf{x})|)^{\frac{-1}{5}} |kH_{u_{\mathcal{M}}}(\mathbf{x})|$$

$$\mathcal{D}_{L^1} = N^{\frac{2}{3}} \left(\int_{\Omega} det(|kH_{u_{\mathcal{M}}}(\mathbf{x})|)^{\frac{2}{5}} \, \mathrm{d}\mathbf{x} \right)^{\frac{-2}{3}}.$$

Hessian-based adaptation

$$\mathcal{M}_{L^1,opt}(\mathbf{x}) = \mathcal{K}_1(1, u_{\mathcal{M}})$$

Goal-Oriented adaptation

$$\mathcal{M}_{opt,goal} = \mathcal{K}_1(|\rho(H(u^*_{g,\mathcal{M}}))|, u_{\mathcal{M}}).$$

Norm-Oriented adaptation

$$\mathcal{M}_{opt,norm} = \mathcal{K}_1(|\rho(H(u^*_{DeC}))|, u_{\mathcal{M}})$$

IV. Applications : Adaptive FMG

The mesh adaptation loop is applied as an **intermediate loop** between:

- the FMG phases loop and
- the MG cycling.

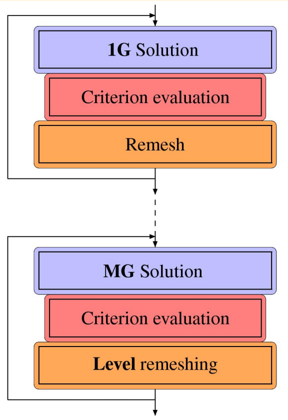

Numerical examples: test case 1

Boundary layer

$-\Delta u = rhs$ with $rhs(x,y) = \frac{1}{\alpha^2(exp(1/\alpha)-1)} exp(x/\alpha)$; $\alpha = 0.03$.

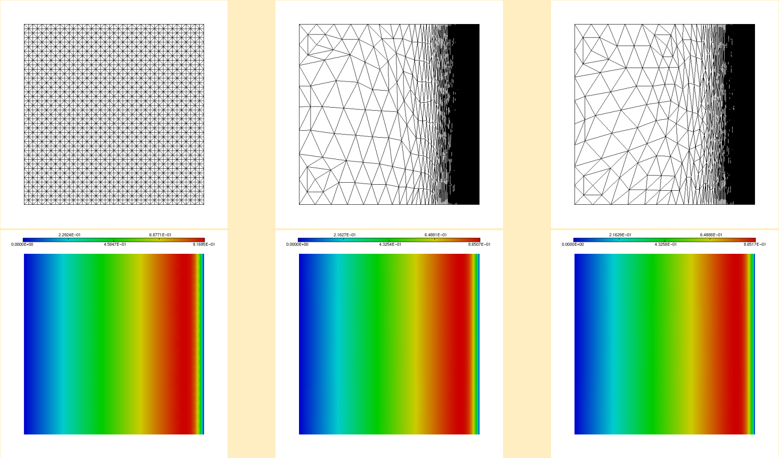

Uniform | Hessian-based | Norm-oriented

Numerical examples: test case 1

Boundary layer

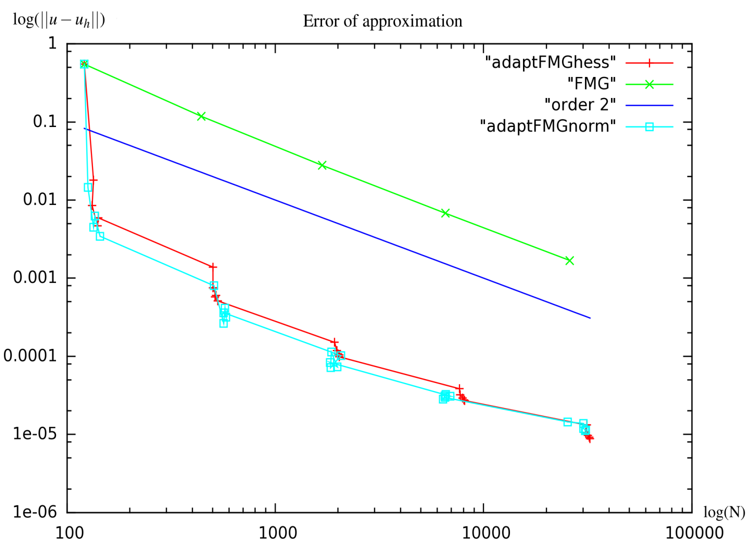

Numerical examples: test case 2

One circle-shaped quasi-discontinuity

We solve $-\Delta u = rhs$ where $u(x,y) = \frac{1}{2}[1 + \frac{2\psi}{\epsilon} + \frac{1}{\Pi} sin(\frac{2\Pi\psi}{\epsilon})]$ with $\psi = R - \sqrt{(x_C - x)^2 + (y_C - y)^2}$ and $\epsilon = 0.02$.

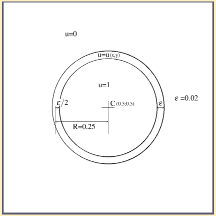

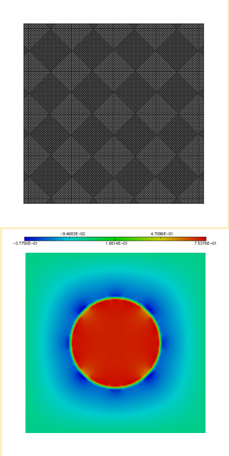

Uniform

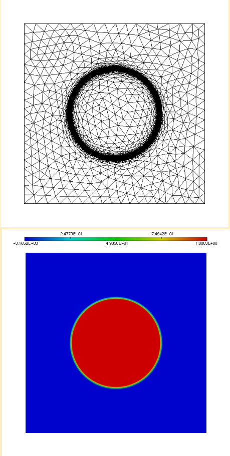

Norm-oriented

Numerical examples: test case 2

One circle-shaped quasi-discontinuity

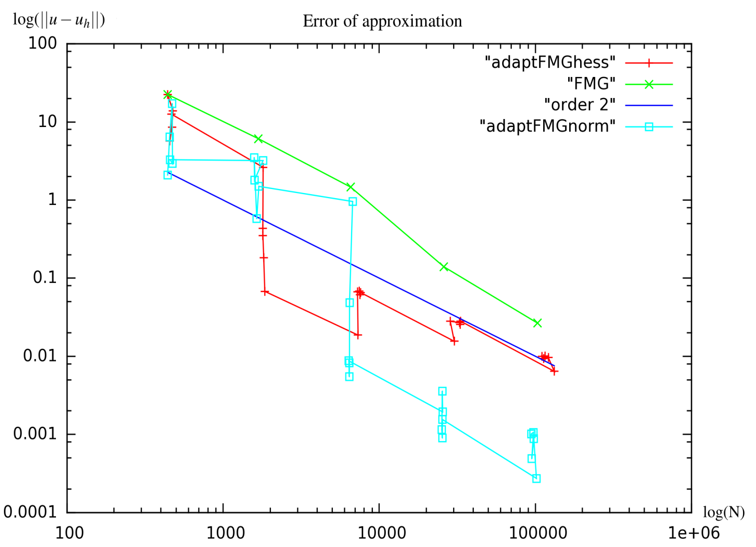

Numerical examples: test case 3

Three circle-shaped quasi-discontinuities

We solve $-\Delta u = rhs$ where $u_i(x,y) = \frac{1}{2}[1 + \frac{2\psi_i}{\epsilon} + \frac{1}{\Pi} sin(\frac{2\Pi\psi_i}{\epsilon})]$ with $\psi_i = R - \sqrt{(x_{C_i} - x)^2 + (y_{C_i} - y)^2}$ and $\epsilon = 0.02$.

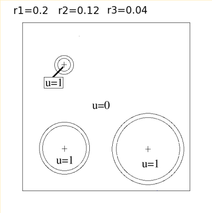

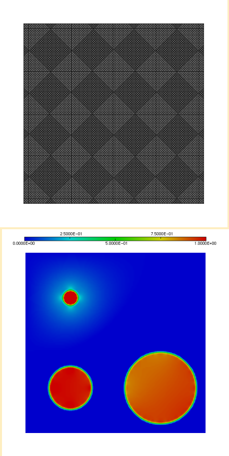

Uniform

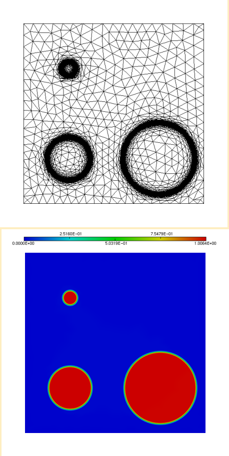

Norm-oriented

Numerical examples: test case 3

Three circle-shaped quasi-discontinuities

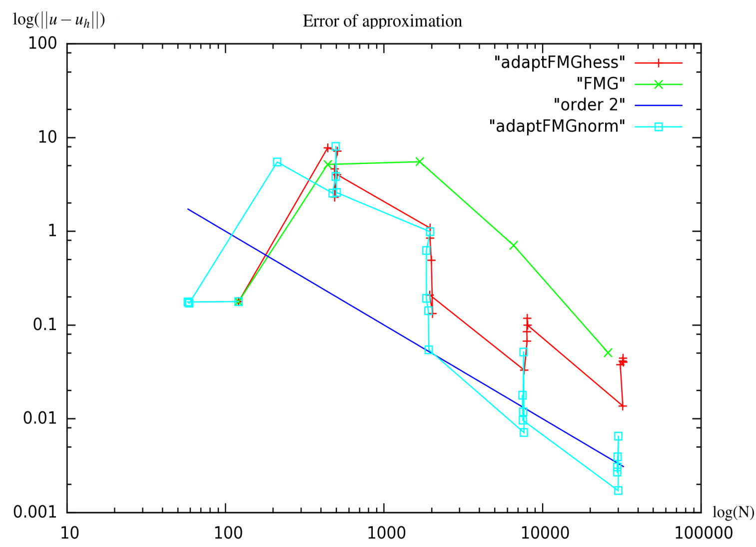

Extension to the Euler system of CFD

We consider the steady Euler system
$F(W)_x + G(W)_y + H(W)_z = 0$ with $W = (\rho, \rho\mathbf{U}, \rho E)$
Approximated with an upwing finite-volume on unstructured mesh.

The corrector is obtained by Defect Correction.

A detailed *a priori* analysis combined with corrector and adjoint is used for norm-oriented mesh adaptation.

A test case: high-lift geometry

First AIAA CFD High Lift Prediction Workshop (Configuration 1).

Three adaptation strategies are compared:
- the first one controls the interpolation error on the density, velocity and pressure in L^1 norm,
- the second controls the interpolation error on the Mach number while
- the third one is based on the norm-oriented approach and controls the norm of the approximation error $||W - Wh||_{L^2}$.

For each case, five adaptations at fixed complexity are performed for a total of 20 adaptations with the following complexities: 160 000, 320 000, 640 000, 1 000 000.

Hessian-based adaptation for minimizing the L^1 norm of the interpolation error on the density, velocity and pressure.

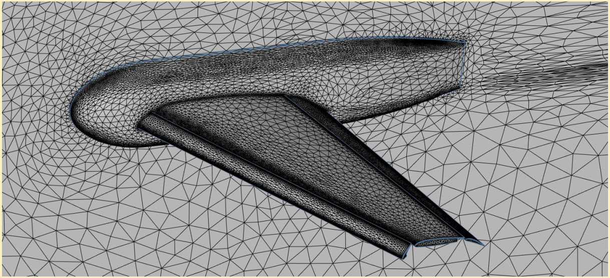

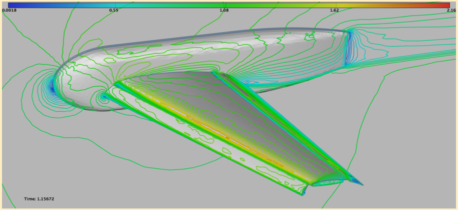

There is not much mesh concentration on the body in the wake of wing. The wake after the body is refined.

Hessian-based adaptation for minimizing the interpolation error on Mach number.

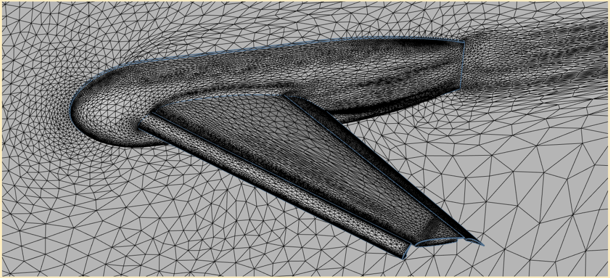

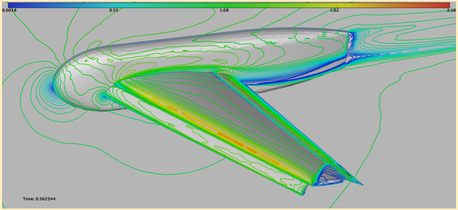

There is a better mesh concentration on the body in the wake of wing. The wake after the body is further refined.

Adaptation for minimizing the norm $||W - Wh||_{L^2}$ with the novel norm oriented approach.

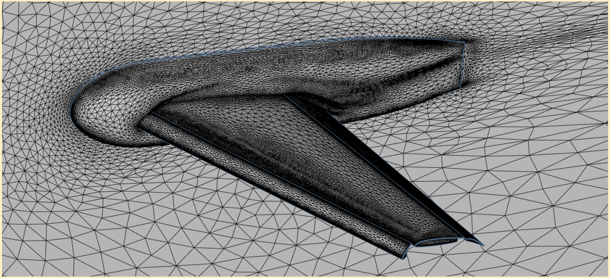

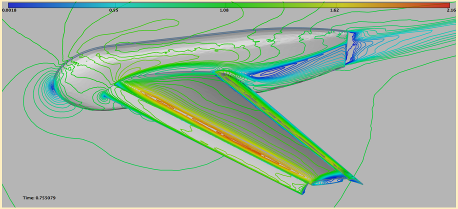

Near-body mesh is finer and show much more details on the aircraft body.

Conclusions

- Hessian-based adaptation
- Goal-Oriented adaptation
- Norm-Oriented adaptation

- Combination of FMG and anisotropic mesh adaptation.

- Novel Norm-Oriented adaptation more robust than Hessian-based adaptation.